ARTICLE OPEN

Check for updates

Strategy to minimize bending strain interference for flexible acoustic wave sensing platform

Jian Zhou[1], Zhangbin Ji[1], Yihao Guo[1], Yanghui Liu[1], Fengling Zhuo[1], Yuanjin Zheng[2], Yuandong(Alex) Gu[3], YongQing Fu[4] and Huigao Duan[1,5]✉

There are great concerns for sensing using flexible acoustic wave sensors and lab-on-a-chip, as mechanical strains will dramatically change the sensing signals (e.g., frequency) when they are bent during measurements. These strain-induced signal changes cannot be easily separated from those of real sensing signals (e.g., humidity, ultraviolet, or gas/biological molecules). Herein, we proposed a new strategy to minimize/eliminate the effects of mechanical bending strains by optimizing off-axis angles between the direction of bending deformation and propagation of acoustic waves on curved surfaces of layered piezoelectric film/flexible glass structure. This strategy has theoretically been proved by optimization of bending designs of off-axis angles and acoustically elastic effect. Proof-of-concept for humidity and ultraviolet-light sensing using flexible SAW devices with negligible interferences are achieved within a wide range of bending strains. This work provides the best solution for achieving high-performance flexible acoustic wave sensors under deformed/bending conditions.

npj Flexible Electronics (2022)6:84 ; https://doi.org/10.1038/s41528-022-00217-0

INTRODUCTION

Surface acoustic wave (SAW) technology[1–3] has been extensively applied for signal processing in wireless communication systems, physical[4,5], chemical[6,7], or biological sensors[8,9], acoustofluidics and lab-on-a-chip[10–12]. Recently, flexible SAW sensors receive substantial interest for mechanically robust, wearable, and adaptive sensing microelectronics, due to their excellent flexibility/foldability, compact size, and wireless capability for in-situ, continuous, and non-invasive monitoring of target parameters. In the past decade, numerous studies on high-performance flexible and bendable SAW sensors have been done for various applications, including temperature sensors[13,14], humidity sensors[15,16], ultraviolet (UV) sensors[17,18], strain sensors[19–23], respiration monitoring[24] and biosensors[9]. For these flexible SAW sensors, flexibility and bendability are the key properties on the curved and bent surfaces. However, there is always a major issue that severe mechanical strains (or bending strains) applied on the flexible SAW devices cause significant frequency shifts, which strongly interfere with the real sensing signals (e.g., humidity, UV, biological species, or gas molecules), thus causing poor accuracy and low sensitivity of these sensors. To solve this issue, reference samples are often deployed to minimize the bending effects, but this results in a complex sensing platform for the detection system. To create a reliable and precise sensing platform, it is essential to develop a new methodology (e.g., using a device-level design) to eliminate the bending strain-induced signal changes for these flexible SAW devices, and to reveal signals only generated from the targeted monitoring parameters. However, up to now, there are few studies, which are focused on this challenge.

In this paper, we propose a new strategy to achieve this objective. It is based on a new phenomenon recently observed, in which frequency shifts of thin film aluminum nitride (AlN) SAW devices on a flexible glass substrate are changed from positive values (Fig. 1a) into negative ones (Fig. 1b) when the off-axis bending angles α between directions of bending deformation and those of acoustic wave propagation are changed from 0° or 90°. Inspired by this new observation, in this study, we established a new approach to achieve a zero-sensitivity of strain or bending insensitivity (as shown in Fig. 1c) by optimizing the off-axis angle on the flexible SAW device, and the mechanisms were thoroughly investigated. In this new methodology, we used a piezoelectric film/flexible glass layered structure, which has been bent with an optimized off-axis angle to minimize the bending strain effects. To achieve this, we firstly developed a theoretical model (Fig. 1d) using a boundary condition method and coupled wave equations to study frequency shifts of devices under an off-axis bending. Based on these theoretical analysis results, we predicted that there is a universal phenomenon of minimizing the bending strain effect by using off-axis bending designs for various flexible SAW devices. The variations in the strain sensitivity of SAW devices with different wavelengths and thicknesses of piezoelectric materials were systematically studied. We then explored the effects of initial stress, elastic constant, density, and interdigital transducer (IDT) deformation (all of which we have identified as the key factors leading to dramatic changes in SAW frequency) on the variations of frequency responses under an off-axis bending. Flexible SAW devices with AlN/flexible glass layered structures were fabricated, and then the bending insensitivity of the flexible devices was demonstrated experimentally with various off-axis angle designs. We finally performed demonstrations for humidity and UV sensing using the flexible SAW devices, without showing apparent influences by the bending strains.

[1]College of Mechanical and Vehicle Engineering, Hunan University, Changsha 410082, China. [2]School of Electrical and Electronical Engineering, Nanyang Technological University, Singapore 639798, Singapore. [3]Shanghai Industrial μTechnology Research Institute (SITRI), 235 Chengbei Rd, Shanghai 201800, China. [4]Faculty of Engineering and Environment, Northumbria University, Newcastle upon Tyne NE1 8ST, United Kingdom. [5]Greater Bay Area Institute for Innovation, Hunan University, Guangzhou 511300, China. ✉email: duanhg@hnu.edu.cn

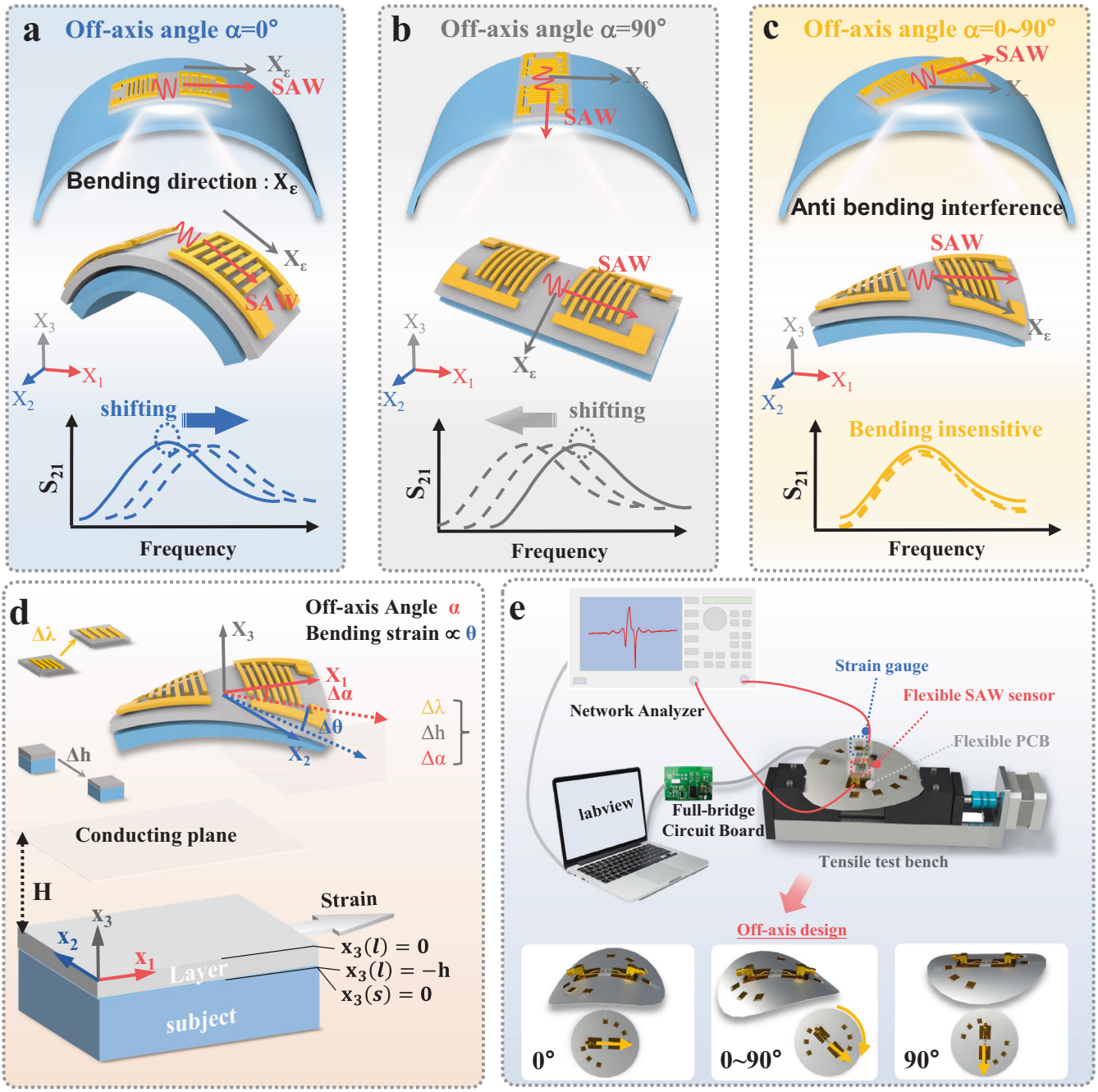

Fig. 1 Structure and strain-unperturbed performance of surface acoustic wave sensor and testing platform for SAW devices. Diagram of strain frequency response SAW sensor with bending states at the off-axis angles of (**a**) 0°, (**b**) 90°, and (**c**) a certain angle with strain-unperturbed characteristic; (**d**) Design and analysis model of the flexible surface acoustic wave sensor with strain-unperturbed characteristic; (**e**) Schematic illustration of strain testing method under flexible bending conditions.

RESULTS AND DISCUSSION

Theoretical analysis of flexible SAWs under off-axis bending

The shifts of resonant frequencies for acoustic wave devices at different bending strains are mainly caused by the changes in wave velocity (i.e., acoustic elastic effect) and device wavelength (i.e., deformation of interdigitated transducers, or IDTs), if we ignore the apparent changes in materials properties except for elastic ones. The overall frequency shift of the flexible acoustic wave devices can be calculated by combining these two effects. The above two components are considered independently in this study, to obtain the frequency shifts of layered acoustic wave devices with different off-axis bending conditions.

Figure 1d schematically illustrates the theoretical model of the proposed flexible SAW sensor, in which α refers to the off-axis angle between the direction of SAW propagation and direction of bending strain. The relative change of wavelength (Δλ/λ) is considered to be equal to the strain in the direction of SAW propagation, which is mainly resulted from the IDT deformation, expressed as $\varepsilon_x = \varepsilon \cos \alpha$. We should address that stress which is perpendicularly applied to the wave propagation direction also induces the device's deformation, which is mainly caused by the

Poisson ratios of the material. However, this effect is commonly known as insignificant. In this study, in order to investigate the influence of the wavelength of the device, we only consider the strain component along the wave propagation direction[20].

The variations of acoustic wave velocities with external stresses can be obtained using an equation, which takes into account the variations of the applied strains.[25] Under a bending strain, the coupling wave equations of a flexible SAW device with a layered structure are[26]

$$\sigma_{jk}\frac{\partial^2 u_i}{\partial x_j \partial x_k} + C_{ijkl}\frac{\partial^2 u_k}{\partial x_l \partial x_j} + e_{jkl}\frac{\partial^2 \phi}{\partial x_k \partial x_j} = \rho\frac{\partial^2 u_i}{\partial t^2} \quad (1)$$

$$e_{jkl}\frac{\partial^2 u_k}{\partial x_l \partial x_j} - \varepsilon_{jk}\frac{\partial^2 \phi}{\partial x_k \partial x_j} = 0 \quad (2)$$

where σ_{jk} is the initial stress; e_{jkl}, C_{ijkl}, and ε_{jk} are piezoelectric constants, elastic stiffness constants, and dielectric constants, ρ is the density; ϕ is the electrical potential; u is the mechanical displacement; and $i, j, k, l = 1, 2, 3$. Solutions of Eqs. (1) and (2) are assumed to follow the standard complex traveling-wave form[25]

$$u_k = e^{j\omega t}\beta_k \exp\left[-j\frac{w}{v}(x_1 + \gamma x_3)\right](k = 1, 2, 3) \quad (3)$$

$$\phi = e^{j\omega t}\beta_4 \exp\left[-j\frac{w}{v}(x_1 + \gamma x_3)\right] \quad (4)$$

where γ is the exponential decay constant in direction x_3, v is SAW velocity, and w is the steady-state angular frequency. For convenience, a four-dimensional displacement vector is defined by letting $u_4 = \phi$.

If we substitute Eqs. (3) and (4) into Eqs. (1) and (2), the Christoffel equation can be obtained[27]. For the different types of materials and different tangential directions of crystals, the Christoffel equations of piezoelectric layer (L) and substrate layer (S) should be listed separately[23,27]. For a layered SAW device, the boundary conditions for the substrate and piezoelectric layer are provided in the supporting information (SI) material (Supplementary Note 1).

The applied strain, which is a perturbation for the propagating waves, will not only change motion equations, but also change the constants of materials. Under the stress, there are three major independent factors, which affect the acoustic velocities, i.e., material elastic constants (C_{ijkl}), initial stress (σ_{jk}), and material density (ρ)[26]. In the calculation process, we replaced these new parameters with the original ones and then calculated the changes of velocities under different off-axis angles and strains. In this work, a program based on MATLAB was applied to calculate the surface acoustic wave velocity as a function of strain.

The frequency shift (Δf) of the flexible acoustic wave devices can be calculated by combining the above two effects, i.e.,

$$\Delta f = (\Delta v/v - \Delta\lambda/\lambda) \cdot f_0 \quad (5)$$

where f_0 is SAW device's intrinsic frequency without any strain. To design strain-insensitive flexible SAW devices, we use the iterative method to optimize the off-axis angles which can reach the minimum value of frequency shift (e.g., close to zero $\Delta f \approx 0$).

In addition, we change the thickness of the piezoelectric film (h) in the boundary conditions set, adjust the wave vectors according to different wavelengths (λ), and obtain the off-axis angle (α) of strain insensitive characteristics of SAW devices with different thicknesses or different wavelengths by repeating the above calculations. Furthermore, we calculate and obtain their respective contributions to the frequency shift (Δf) under different strains. The corresponding values of strain sensitivity ($S = \Delta f/\Delta\varepsilon$) under different off-axis angles are also obtained by separately modifying the three perturbed factors including σ_{ij}, C_{ijkl}, and ρ. Using the above models, we have studied the effects of the thickness of piezoelectric film and wavelength of SAWs on the strain sensitivity of SAW devices, and then explain the mechanism behind this effect.

Strain-insensitive characteristics

Figure 2a shows the theoretical frequency-strain responses of a flexible AlN/glass layer SAW with a 24 μm wavelength (λ) and 1.2 μm thickness as functions of the off-axis angle and bending strain. It clearly shows that, with the increase of off-axis angles from 0 to 70°, the frequency shift (deduced by the strain) of the flexible SAW devices is decreased significantly. There exists a specific off-axis angle, e.g. ~70°, at which a zero-sensitivity of strain can be obtained, which indicates that there is a bending insensitivity case for the AlN acoustic wave device on the flexible glass. We further investigated responses of frequencies at different strains for the flexible ZnO/glass devices (with a wavelength λ of 40 μm and a ZnO layer thickness of 1 μm) as functions of both bending strains and off-axis angles. When the off-axis angle is close to 45°, this flexible ZnO/glass-based SAW device can also achieve the zero-sensitivity to strain or the bending insensitivity, as shown in Fig. 2b.

We have further changed the substrate material and found that this phenomenon of strain-insensitivity can also be observed on flexible Al foil-based SAW devices (e.g., AlN/Al foil and ZnO/Al foil SAW devices), and the obtained results are shown in Fig. 2c & d for these flexible SAW devices.

These results demonstrate that the bending insensitivity is a universal phenomenon for the layered structure-based flexible SAW devices, and different SAW structures have their unique off-axis angles to achieve this bending insensitivity effect.

We then further calculated the dependence of strain sensitivity of the acoustic wave devices upon the off-axis angles by considering three key parameters (i.e., density, initial stress and elastic constant), all of which result in significant variations in the SAW velocities. We also calculated the effects of IDT deformation (e.g., variation in IDT dimensions in the direction of SAW propagation) on the strain sensitivity. Furthermore, the combined influence of the above four factors on strain sensitivity of the flexible SAW was also systematically investigated.

Figure 2e shows the obtained results for flexible AlN/glass layered SAWs with a wavelength λ of 24 μm and an AlN layer thickness of 1.2 μm. When α is 0°, the stresses and density changes of materials generate a positive strain sensitivity, whereas the deformed IDTs and the change of elastic constant generate a negative strain sensitivity. The combined effect of these two opposite outputs leads to a positive strain sensitivity. This is because the initial stress is the key contributing factor, whereas the density contribution has a minimum effect. However, results show that if the off-axis angle is changed between 0° and ~70°, the independent contributions of these factors to the strain sensitivity are all changed. The strain sensitivity is decreased in a linear relationship because of the reasons mentioned above, and the AlN acoustic wave device on the flexible glass shows a zero-strain sensitivity when the value of α is increased up to ~70°. The ZnO/flexible glass-based SAW device (with a wavelength λ of 40 μm and a ZnO layer thickness of 1 μm.) has a similar trend to that of the AlN film/glass-based acoustic wave device, as shown in Fig. 2f. When the off-axis angle α is changed from 0° to ~45°, the strain sensitivity of the ZnO/glass SAW device is decreased with nearly a linear relationship due to the combined effects of all the above four factors, and a zero-strain sensitivity can be achieved with the off-axis angle α of 45°. The initial stress is still identified as the key factor for achieving this.

For the Al foil-based flexible SAW devices (Fig. 2g and h), the largest contribution to the strain sensitivity is the change of elastic constant but not its initial stress. Therefore, the strain sensitivity is a negative value when the off-axis angle α is 0°. With the off-axis angle α increased, the strain sensitivity caused by the change of

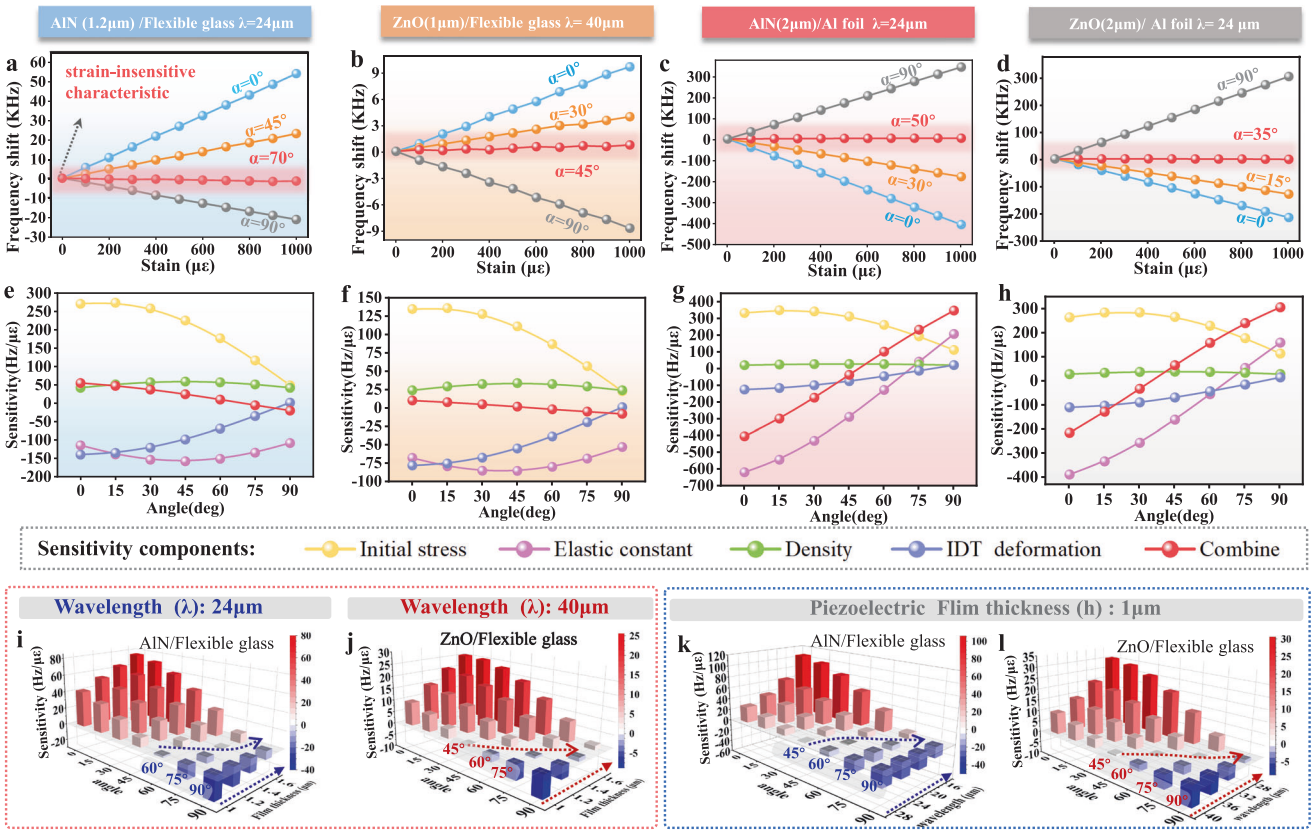

Fig. 2 strain-insensitive characteristic numerical calculation results. Frequency shift of SAW devices as a function of applied strain in the range of 1000 με at different off-axis angles which are based on (**a**) AlN/flexible glass, (**b**) ZnO/flexible glass, (**c**) AlN/Al foil and (**d**) ZnO/Al foil, respectively; Theoretical calculated dependence of strain sensitivity (which is caused by density, elastic constants, initial stress, and deformation of IDTs) on off-axis angles, for (**e**) AlN/flexible glass, (**f**) ZnO/flexible glass (**g**) AlN/Al foil and (**h**) ZnO/Al foil respectively; Strain sensitivities of acoustic wave devices with the changes of off-angle at different piezoelectric film thicknesses, which are based (**i**) AlN/flexible glass and (**j**) ZnO/flexible glass; Strain sensitivities of acoustic wave devices with the changes of off-angles at various interdigital periods, which are based (**k**) AlN/flexible glass and (**l**) ZnO/flexible glass.

elastic constant is significantly decreased, thus the strain sensitivity is gradually changed from a negative value to a positive one.

For these thin-film SAW devices, this specific off-axis bending angle for achieving bending insensitivity is not only related to the material itself but also affected by the thickness of the piezoelectric film and the wavelength of the SAW device, which will be discussed in the next section.

Figure 2i shows the effects of piezoelectric film thickness on the off-axis angles with zero strain sensitivity for an AlN/flexible glass-based SAW device with a wavelength of 24 μm. Results show that, for a fixed off-axis angle, with the thickness of AlN film increased from 1 μm to 1.6 μm, the strain sensitivity is gradually increased. Whereas the off-axis angle which can achieve the zero strain sensitivity is increased from ~60° to ~90° when the thickness of AlN film is increased from 1 μm to 1.6 μm. Similarly, with the increase of film thickness from 1 μm to 1.6 μm, the off-axis angle with zero strain-sensitivity for ZnO/flexible glass-based SAW device (wavelength of 40 μm) is increased from ~45° to ~90°, as shown in Fig. 2j. These results indicate that, when the wavelength of a flexible SAW device is fixed, an increase in the piezoelectric film thickness will increase the off-axis angle at which a zero strain sensitivity can be obtained.

We further study the influence of wavelength on the strain sensitivity and the off-angle with a zero strain sensitivity. The sensitivity of strain for flexible acoustic wave devices (with an AlN film thickness of 1 μm) with different wavelengths has been calculated, and the obtained results are shown in Fig. 2k. It is clear that with the wavelength decreased from 28 μm to 16 μm, the strain sensitivity of AlN acoustic wave devices is increased, whereas the off-axis angle with zero strain sensitivity is increased from ~45° to ~90°. Similarly, for the ZnO/flexible glass-based SAW, it shows the same trend (Fig. 2l), which further confirms that decreasing the wavelength increases the strain sensitivity and thus the off-axis angle at which the zero strain sensitivity can be obtained.

The main reason for this phenomenon can be explained as follows. When the piezoelectric film thickness is increased or the wavelength is decreased, more acoustic wave energy is concentrated within the piezoelectric film. As the stiffness values of the AlN and ZnO piezoelectric films (Supplementary Table 1) are much larger than that of the ultra-thin glass, larger stress is generated in the piezoelectric film, under the same applied bending strain. Therefore, much more energy is concentrated in the piezoelectric film, and the effect of the initial stress on the changes of acoustic velocity becomes more significant as shown in Supplementary Fig. 1a & b. Accordingly, the decrease rate of the positive SAW velocity becomes smaller.

The change of elastic constant under the applied bending strain, which is another key reason affecting the change of SAW velocity, is mainly determined by the higher-order elastic constant of the ultra-thin glass substrate and piezoelectric film. It is worth noting that the third-order elastic modulus of AlN or ZnO can be ignored because the bonding between microcrystals in polycrystalline films is very weak, which has been well-explained in ref. [25]. Therefore, when the acoustic energy is more concentrated

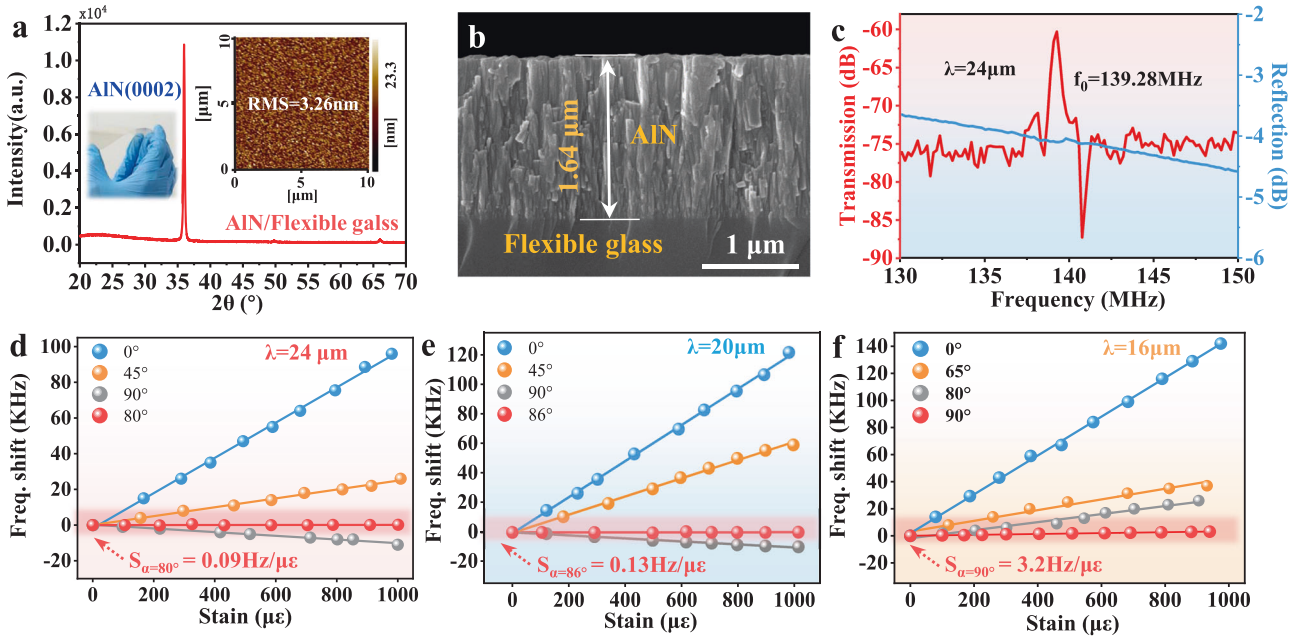

Fig. 3 Experimental validation of AlN(1.64 μm)/flexible glass-based flexible SAW device for the strain-unperturbed behavior. a XRD pattern and photographs of the AlN/glass, exhibiting strong (0002) orientation and good flexibility, and the inset is its AFM image displaying a smooth surface; (**b**) SEM image of its cross-section; (**c**) Transmission and reflection of the flexible AlN/glass-based SAW device. **d–f** Resonant frequency of flexible AlN/glass-based SAWs at λ = 24 μm, 20 μm, and 16 μm, varying with bending strain at different off-axis angles α.

in the piezoelectric film, the negative contribution of the elastic constant to the change of acoustic wave velocity will be decreased (Supplementary Fig. 1a & b), which leads to the smaller decrease rate of the positive SAW velocity. Accordingly, when the piezoelectric film thickness is increased or the wavelength is decreased, the decreased rate of SAW velocity becomes smaller for AlN or ZnO on ultra-thin glass devices, which leads that a higher off-axis angle is needed to compensate for the negative contribution of IDT deformation and achieve minimizing bending strain influences.

For the Al foil-based flexible SAW devices, decreasing the wavelength or increasing the thickness of piezoelectric film decreases the off-axis angle with zero strain sensitivity as shown in Supplementary Fig. 2a–d. This is opposite to the trends for the AlN/glass SAW devices. This is because, for these Al foil-based SAW devices, the largest contribution is the elastic constant but not the initial stress, and the strain sensitivity becomes negative at the off-axis angle of 0°. With the decrease of wavelength or increase of thickness of the piezoelectric film, more acoustic wave energy is concentrated in the piezoelectric film. Therefore, the contribution of initial stress to the positive change of acoustic velocity becomes more significant, whereas the contribution of elastic constant which leads to the negative strain-sensitivity becomes much weaker. Therefore, the increase rate of SAW negative velocity becomes much larger, and thus the zero strain-sensitivity can be achieved at a much smaller off-axis angle.

To sum up, to realize the strain insensitivity characteristic of the flexible SAW devices, it is critical to control the values of elastic constant, density, initial stress, and IDT deformation (e.g., these four key factors mainly cause the changes of frequency). In addition, most of the SAW energy is confined within the near-surface region of the substrate, especially for the piezoelectric film/flexible substrate layered SAW devices. Therefore, both the types of substrate and its material parameters are important factors for strain insensitivity characteristic of the flexible SAW devices, which were detailed discussed in the Supporting Information material(Supplementary Discussion 1).

Validation of the strain-insensitivity for flexible devices

ZnO and AlN are two commonly used piezoelectric films for preparing thin-film SAW devices. The advantages of AlN film if compared with ZnO film is its high acoustic velocity, and thus it is more suitable for high frequency and high precision SAW sensing applications[28]. The AlN film also has the advantage of good compatibility with complementary metal-oxide-semiconductor (CMOS) technologies. Whereas it is commonly known that ZnO is not good as Zn is regarded as an unwanted contamination dopant for CMOS[29]. What's more, the AlN film has better chemical stabilities and is the suitable candidates for high-performance sensors for applications in acidic/alkali and high-temperature environments[30]. For these reasons, we have selected and fabricated AlN-based flexible SAW devices for validation of the strain-insensitive flexible devices.

AlN films with a preferred vertical orientation and an average stress value of ~36.83 MPa (which was obtained from X-ray diffraction or XRD analysis) were deposited onto flexible glass substrates using a magnetron sputter [22] (Fig. 3a). XRD spectrum presents a single peak at 2θ = ~36° and a full width at half maximum value of 0.257°, indicating that it has a dominant c-axis orientation. The inset image in Fig. 3a shows the surface morphology of the AlN films measured with an atomic force microscope (AFM). On a flexible glass substrate, the surface of AlN is quite smooth with a measured root means square roughness (RMS) of ~3.26 nm, within an area of 10 × 10 μm^2. Figure 3b presents a cross-section scanning electron microscope (SEM) image of AlN film on the flexible glass. The film thickness is 1.64 μm and the vertically columnar structure is observed, demonstrating the c-axis orientation of AlN film, which is consistent with the XRD results.

UV photolithography and lift-off processes were used to pattern the IDTs (5 nm Cr/40 nm Au) and prepare AlN acoustic wave devices with wavelengths of 24, 20, and 16 μm. Its transmission (S_{21}) parameters acquired by a network analyzer are shown in Fig. 3c and Supplementary Fig. 3 a & b. There are obvious Rayleigh resonant peaks at 139.28, 168.13, and 211.77 MHz with IDT wavelengths of 24, 20, and 16 μm, respectively.

The fabricated SAW devices were bonded onto a 0.1 mm thick spring steel plate and then electrically connected to the flexible printed circuit board (PCB), as shown in Supplementary Fig. 4a. A tensile tester was used to bend the steel plate and apply the bending strain to the flexible SAW device. Supplementary Fig. 4b & c shows the cross-section images of the flexible SAW device in a flat state (Supplementary Fig. 4b) and on the curved steel plate (Supplementary Fig. 4c).

Frequency-strain responses of AlN flexible acoustic wave devices are shown in Fig. 3d, at different bending strains and off-axis angles, with λ of 24 μm and AlN thickness of 1.64 μm. The measured values of frequency-strain sensitivity are 98.74, 24.86, 0.09, and −9.94 Hz/με at various off-axis angles of 0, 45, 80, and 90°, respectively. It is clear that with an off-axis angle of 80°, the frequency-strain sensitivity is obtained as near zero, i.e., with a value of only ~0.09 Hz/με, which is consistent with the theoretical result (Supplementary Fig. 5a, ~83° to achieve the zero strain sensitivity). Figure 3e & f shows the experimentally obtained frequency-strain responses at λ = 20 and 16 μm as well as with an AlN thickness of 1.64 μm. The measured strain sensitivity is 0.13 Hz/με for the flexible SAW with λ of 20 μm and an off-axis angle of 86°. While the strain sensitivity is 3.2 Hz/με for the flexible SAW device with λ of 16 μm and an off-axis angle of 90°. These are consistent with theoretical results as shown in Supplementary Fig. 5 b & c.

In addition, with the wavelength of the SAW device decreased from 24 to 20, and then to 16 μm, the off-axis angle to achieve the zero strain sensitivity is increased from 80° to 86°, and then to 90°, demonstrating that the decrease of the wavelength increases the off-axis angle for achieving a zero strain-sensitivity. These experimental results are consistent with those of simulation ones. Supplementary Fig. 6 presents frequency-strain responses of the AlN/glass acoustic wave device as functions of both off-axis angles and bending strain, with a wavelength of 20 μm and an AlN film thickness of 1.2 μm. The off-axis angle for zero strain sensitivity is about 75°, which is lower than the value of 86° for the SAW device with the AlN thickness of 1.64 μm and the same wavelength. This indicates that a thicker piezoelectric film will cause a larger off-axis angle to achieve the zero strain sensitivity, which is same with those of the theoretical results.

All these experimental results verified that there exist the strain insensitive properties of acoustic wave devices when the optimized off-axis bending angles have been applied, and also this angle of strain insensitivity of flexible SAW devices is a function of wavelengths of SAW and thicknesses of piezoelectric materials.

We further did experiments to verify that the strain insensitive properties of the proposed SAW can also occur in the SAW device under the concave bending. The obtained results for the SAW device with λ = 24 μm and AlN thickness of 1.64 μm are shown in Supplementary Fig. 7a. It clearly shows that at an off-axis angle of ~81°, the frequency-strain sensitivity is near to zero, with a value of only ~0.7 Hz/με. This is consistent with the theoretical results shown in Supplementary Fig. 7b (which is at ~84° for achieving the zero strain sensitivity under the concave bending conditions). We can confirm that for the concave bending, the strain insensitive properties are similar to those under the convex bending, and there exists a certain value of off-axis angle at which the flexible SAW device is insensitive to the bending strain.

Finally, to investigate the stability and fatigue failure of flexible SAW devices for real-life applications, the flexible SAW device (with a wavelength λ of 20 μm abd an AlN thickness of 1.64 μm) was repeatedly bent/released for more than 100 cycles with a maximum applied strain of 800 με and an off-axis angle of 0°. Supplementary Fig. 8 shows that the maximum frequency shift of the overall bending test is slightly less than ~0.7 KHz and the relative deviation is less than 1.1%, indicating that the performance of the flexible SAW device (e.g., frequency shifts) does not shown apparent degradation. These results verify that the fabricated flexible SAW device has good mechanical durability and stability, demonstrating its great potentials for flexible electronics applications.

Proof-of-concept for sensing applications

Humidity sensing and UV detection were conducted to demonstrate the strain-insensitivity of the flexible SAW sensors. The obtained results are shown in Fig. 4. In order to show that different types of flexible SAW devices can all minimize the bending strain effects, we used three types of devices with different wavelengths or film thicknesses for demonstrations, i.e. two SAW devices with a wavelength λ of 20 μm and AlN thickness of 1.64 and 1.2 μm for humidity test, and a SAW device with λ of 16 μm and AlN thickness of 1.64 μm for UV detection.

Humidity level is an important parameter for our daily life and industrial production. Monitoring of humidity or moisture levels is critical for respiratory equipment[15]. In addition, it is a key indicator of wafer processing for manufacturing integrated circuits in a cleaning room[31]. What's more, monitoring the hydration levels of the skin allows for the evaluation of various human physiological conditions, which can be related to athletic performance[32], aging process[33], and the healing process of wounds[34]. Figure 4a illustrates the humidity sensing set-up using the acoustic wave device bent with a selected off-axis angle at which there is the minimized strain sensitivity. Figure 4b shows the humidity-frequency responses of the flexible SAW sensors (with an λ of 20 μm and AlN thickness of 1.64 μm) as the relative humidity (RH) level was changed from 30% to 70% RH and then back to 30% for five cycles, at different bending strains. Results show that when the SAW device is under 0 με (e.g. mounted on a flat surface without bending), the resonant frequencies of the flexible SAW device are decreased with the relative humidity from 30% to 70% RH, and then returned to their original values as the humidity decreased from 70% to 30% RH for five cycles. The devices show outstanding humidity sensitivity and repeatability. As shown in Fig. 4b, with the increase of bending strain under a normal bending state, the initial resonant frequency of the SAW devices is increased. This means the resonant frequency will be influenced by both bending strain and environment humidity, as it is well-known that frequency changes caused by the bending of the device will influence its sensing capability for humidity sensing on the curved surface.

As shown in Fig. 4c, when the SAW device is bent with an off-axis angle of 86°, the bending strain does not affect the initial frequency of the SAW device. This result clearly demonstrates the device's strain-insensitive characteristics using the novel off-axis angle design. It should be noted that when the SAW device is under the bending state, the response time for the humidity sensing appears to slightly increase, possibly because it needs a longer adsorption time for the water molecule to be adsorbed onto the curved surface. Nevertheless, the response time does not affect the strain sensitivity and frequency shift. We also conducted the small range humidity measurements using the SAW sensor, and the obtained results are shown in Supplementary Fig. 9. Results show that, with an off-axis angle of 86°, the flexible SAW device shows the minimized interference of mechanical bending strains (~600 με), and clearly detects small changes in the ambient humidity (e.g., from ~30% to ~40% RH).

To further study the effect of disturbance of dynamic strain on humidity sensing, different strains were loaded on the flexible SAW (λ of 20 μm, AlN of 1.2 μm) along with the selected off-axis angles during the humidity sensing. The sensing results are shown in Fig. 4d. With the RH level changed from 30 % to 70% at the bending stain of 0 με, the frequency of the flexible SAW is decreased due to the humidity mass-loading. When the acoustic wave device is bent at an RH value of 70%, the resonant frequency

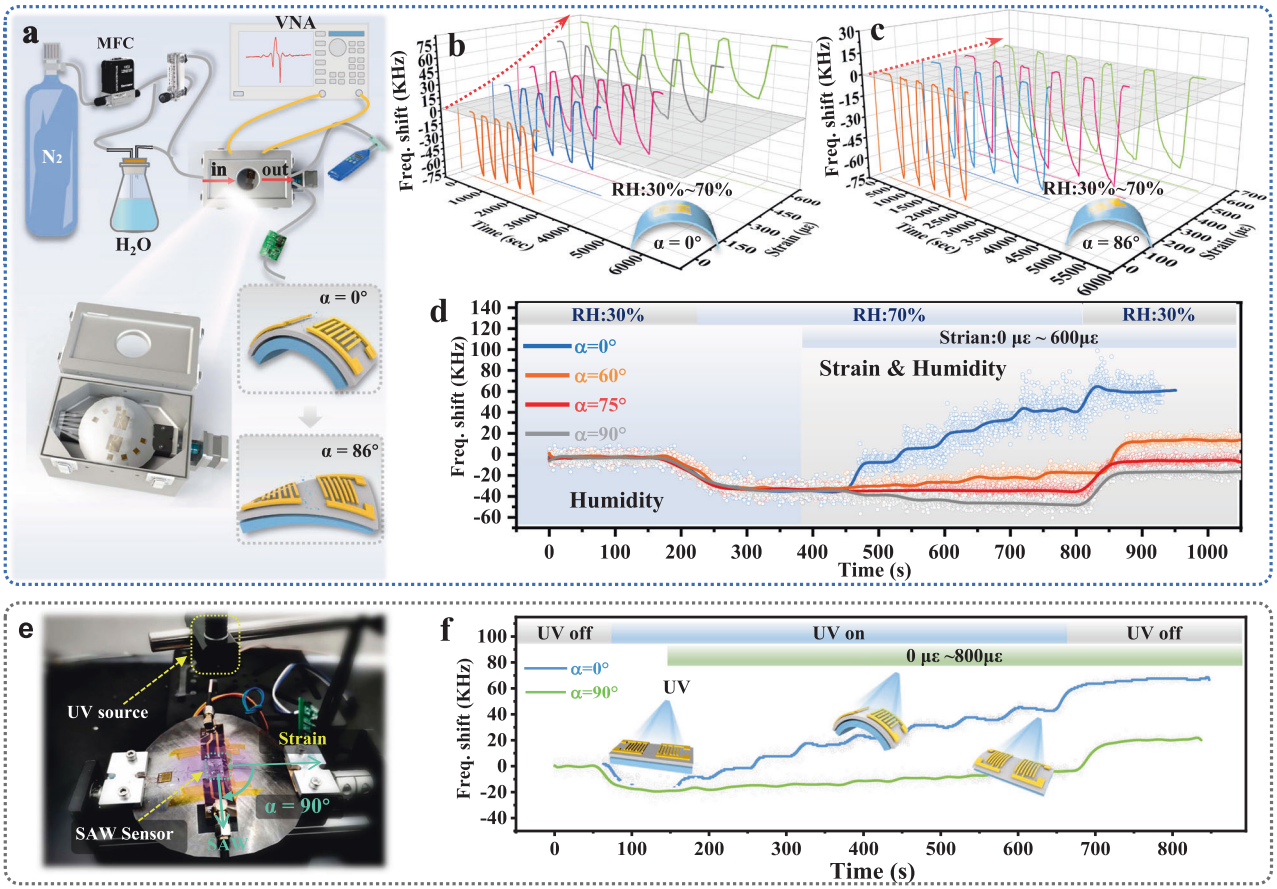

Fig. 4 Flexible SAW sensor with strain-unperturbed characteristic for curved surface sensing applications. a Schematic view of the testing system used for flexible humidity sensing; (**b**) Frequency shifts caused by humidity changed from 30% to 70% RH with five cycles, for the conventional flexible sensors (off-axis angle of 0°) under bending strain from 0 to 600 με; (**c**) Frequency shifts caused by humidity changed from 30% to 70% RH with five cycles, for the novel flexible sensors (off-axis angle of 86°) under bending strain from 0 to 600με, showing the anti-strain interference; (**d**) Comparison of frequency shifts of the flexible sensors with different off-axis angle, for strain response when they were under humidity sensing. **e** Schematic diagram of an experimental setup to detect ultraviolet using the acousitc wave sensor under a normal bending and off-axis bending conditions; (**f**) Comparison of frequency shifts of the flexible SAW sensors with off-axis of 0 and 90° under different dynamic strain (from 0 to 800 με), at the UV intensity changed from 0 to 35 mw/cm^2.

is also shifted for the acoustic wave device with an off-axis angle of 0°, although the humidity environment is unchanged. Applying a larger strain results in a larger resonant frequency shift. However, when the flexible SAW is under bending with an off-axis angle of 75°, the resonant frequency is nearly unchanged even if the flexible SAW device is bent with a strain up to 600 με. Results clearly demonstrate that the acoustic wave devices under an off-axis bending can achieve a strain-insensitive sensing capability for humidity sensing.

We further did UV sensing using the flexible SAW device on curved and complex surfaces to demonstrate the application using this new methodology. UV radiation has a profound influence on human health. For example, sunlight, which contains the UV light, is good for the human body as it enables synthesis of vitamin D, however, excessive exposure to sunlight (mainly UV light) can lead to skin cancer or other diseases[35]. In addition, UV light with a wavelength of 365 nm can inactivate E.Coli and mesophilic bacteria, and has been used in water disinfection.[36,37] Therefore, the detection of UV light can monitor the germicidal efficiency of UV radiation.

The AlN/glass flexible SAW device was used in this case, with a wavelength λ of 16 μm and an AlN layer thickness of 1.64 μm. The surface of the SAW device was covered with ZnO nanowires (bought from XFNANO, Nanjing, China) by a spinning method to improve the absorption of UV light. The SAW device was bonded onto a flat steel plate for the UV detection (wavelength is 365 nm and its intensity is 35 mw/cm^2) at both a flat state and various bent states (with the applied bending strains from 0 to 800 με) (Fig. 4e). Figure 4f shows the comparisons of frequency shifts for the acoustic wave sensors with off-axis angle of 0° and 90°. It is clear that for the case that the off-axis angle was set at 90°, the working frequency was nearly unchanged with different bending strains, showing the strain-unperturbed performance of this sensor. It should be noted that the baseline (after 700 seconds) of the SAW device (off-axis of 90°) seems to be slightly shifted if compared with the initial baseline (t=0 s), mainly because long-term exposure to UV irradiation causes increase of temperature and heat accumulation, which will lead to a slight shift of the resonant frequency (Supplementary Fig. 10). More detailed explanations are provided in our SI materials (Supplementary Discussion 2).

Our flexible SAW devices are mainly consisted of the inorganic material of flexible glass substrate, AlN film and metallic IDTs, all of which are IC compatible. Therefore, these ultra-thin flexible glass-based SAW devices have great potentials for large wafer-level mass production. However, we should also address that due to the brittleness of glass substrate (even though it is flexible in a certain degree), it is difficult for the ultra-thin glass to be signficantly twisted like those of flexible polymer substrates[38]. Therefore, in

the applications, these flexible glass-based SAW devices can be bent or twisted, but should not be deformed significantly.

In this paper, we proposed a new strategy to minimize the bending strain influences on the sensing performance using AlN film/flexible glass layered structure under a bending stress along an off-axis angle on the curved surface. Importantly, we theoretically analyzed the effects of bending or off-axis deformation on frequency shifts by using the boundary condition method with coupling wave equations. Our results proved the universal phenomenon of bending strain insensitive characteristics for layered flexible SAW devices. The mechanisms behind this phenomenon were theoretically studied. In addition, the effects of wavelengths and piezoelectric film thickness on the changes of this off-axis angle for obtaining the zero strain-sensitivity of flexible SAW device were theoretically studied. We then experimentally verified using AlN film/flexible glass layered structure SAW devices. Finally, we experimentally demonstrated the humidity and UV sensing with bending strain insensitive characteristics, exhibiting negligible changes in frequencies due to the various bending strains applied (e.g., 0~600 με for humidity sensing, 0~800 με for UV sensing). Our novel sensing strategy with the optimized off-axis angle bending endows the flexible SAW sensors with the capability of accurately detecting environmental parameters, under complex dynamic strains, but without influence by the bending strains.

METHODS

AlN film characterization

Piezoelectric AlN films were deposited onto flexible glass substrates using a reactive magnetron sputtering system (SVAC-PilmLab-S400, China) with a pure Al target and a gas mixture of N_2/Ar. The crystal orientation of the AlN film was characterized using X-ray diffractometer (XRD, PANalytical Empyrean) with a Cu-$K\alpha$ radiation source and a scanning range of $2\theta = 20°$~$70°$. Crystallite sizes were calculated using the Debye–Scherrer formula based on the full width at half maximum (FWHM) of the AlN diffraction peak: $D = K\lambda/(\beta\cos\theta)$[15], where K is the shape factor of the average crystallite with a value of 0.94, λ is the X-ray wavelength (1.5405 Å for a Cu target), θ is the Bragg angle, and D is the mean crystallite gain size normal to diffracting planes. Scanning electron microscopy (MIRA4 LMH, TESCAN) and atomic force microscopy (Dimension Icon, Bruker) were applied to characterize the cross-sectional morphologies and surface topography of the AlN films.

Fabrication of flexible SAW devices

UV photolithography and lift-off processes were used to pattern the IDTs (5 nm Cr/40 nm Au) and prepare AlN acoustic wave devices with wavelengths of 24, 20, and 16 μm. The acoustic wave devices had IDTs of fifty pairs, and its metallization ratio is 0.5. The number of reflectors is 100, and the aperture width is 200 λ. Its transmission (S21) parameters acquired by a network analyzer (Ceyear 3656D, China, with the maximum frequency up to 20 GHz,).

Strain, humidity and UV sensing setup

For bending strain sensing test, the fabricated SAW devices were bonded onto a 0.1 mm thick spring steel plate and then electrically connected to the flexible printed circuit board (PCB, which was mounted onto a steel plate) using conductive silver paste. A tensile tester was used to bend the steel plate and apply the bending strain to the flexible SAW device. Four standard full-bridge strain gauges were glued onto a steel plate that is close to the SAW sensor to provide strain reference to calibrate the dynamic strain. For UV sensing test, the surface of the SAW device was covered with ZnO nanowires by a spinning method to improve the absorption of UV light. An ultraviolet lamp (NBet Technology Co., Ltd., China) was used to generate UV lights with a fixed UV power (35 mW/cm^2) at a fixed wavelength of 365 nm. For humidity sensing test, The whole device was placed inside an aluminum box for humidity sensing. The flow rate of N_2 through the water bottle was controlled by the glass rotor flowmeter to achieve different humidity conditions. LabVIEW programs were applied to obtain time-domain frequency variations of the SAW device.

DATA AVAILABILITY

The data that support the findings of this study are available from authors of the paper upon reasonable request.

Received: 13 May 2022; Accepted: 8 September 2022;
Published online: 22 September 2022

REFERENCES

1. He, H. et al. Topological negative refraction of surface acoustic waves in a Weyl phononic crystal. *Nature* **560**, 61–64 (2018).
2. Satzinger, K. J. et al. Quantum control of surface acoustic-wave phonons. *Nature* **563**, 661–665 (2018).
3. Munk, D. et al. Surface acoustic wave photonic devices in silicon on insulator. *Nat. Commun.* **10**, 4214 (2019).
4. Zheng, J. P. et al. 30 GHz surface acoustic wave transducers with extremely high mass sensitivity. *Appl. Phys. Lett.* **116**, 123502 (2020).
5. Zhou, J. et al. Record-breaking frequency of 44 GHz based on the higher order mode of surface acoustic waves with $LiNbO_3/SiO_2/SiC$ heterostructures. *Engineering*, https://doi.org/10.1016/j.eng.2022.05.003 (2022).
6. Chen, Z. et al. Ultrahigh-Frequency Surface Acoustic Wave Sensors with Giant Mass-Loading Effects on Electrodes. *ACS Sens* **5**, 1657–1664 (2020).
7. Xiong, S. et al. High Performance Acoustic Wave Nitrogen Dioxide Sensor with Ultraviolet Activated 3D Porous Architecture of Ag-Decorated Reduced Graphene Oxide and Polypyrrole Aerogel. *ACS Appl. Mater. Interfaces* **13**, 42094–42103 (2021).
8. Ji, J. et al. An aptamer-based shear horizontal surface acoustic wave biosensor with a CVD-grown single-layered graphene film for high-sensitivity detection of a label-free endotoxin. *Microsyst. Nanoeng.* **6**, 4 (2020).
9. Lamanna, L., Rizzi, F., Bhethanabotla, V. R. & De Vittorio, M. Conformable surface acoustic wave biosensor for E-coli fabricated on PEN plastic film. *Biosens. Bioelectron.* **163**, 112164 (2020).
10. Gu, Y. et al. Acoustofluidic centrifuge for nanoparticle enrichment and separation. *Sci. Adv.* **7**, eabc0467 (2021).
11. Fu, Y. Q. et al. Engineering inclined orientations of piezoelectric films for integrated acoustofluidics and lab-on-a-chip operated in liquid environments. *Lab Chip* **21**, 254–271 (2021).
12. Tao, R. et al. Hierarchical Nanotexturing Enables Acoustofluidics on Slippery yet Sticky, Flexible Surfaces. *Nano Lett.* **20**, 3263–3270 (2020).
13. Jin, H. et al. Flexible surface acoustic wave resonators built on disposable plastic film for electronics and lab-on-a-chip applications. *Sci. Rep.* **3**, 2140 (2013).
14. Lamanna, L., Rizzi, F., Bhethanabotla, V. R. & De Vittorio, M. GHz AlN-based multiple mode SAW temperature sensor fabricated on PEN substrate. *Sens. Actuators, A* **315**, 112268 (2020).
15. Wu, J. H. et al. Ultrathin Glass-Based Flexible, Transparent, and Ultrasensitive Surface Acoustic Wave Humidity Sensor with ZnO Nanowires and Graphene Quantum Dots. *ACS Appl. Mater. Interfaces* **12**, 39817–39825 (2020).
16. He, X. L. et al. High sensitivity humidity sensors using flexible surface acoustic wave devices made on nanocrystalline ZnO/polyimide substrates. *J. Mater. Chem. C.* **1**, 6210–6215 (2013).
17. Tao, R. et al. Flexible and Integrated Sensing Platform of Acoustic Waves and Metamaterials based on Polyimide-Coated Woven Carbon Fibers. *ACS Sens* **5**, 2563–2569 (2020).
18. Yin, C. S. et al. Enhancing the sensitivity of flexible acoustic wave ultraviolet photodetector with graphene-quantum-dots decorated ZnO nanowires. *Sens. Actuators, A* **321**, 112590 (2021).
19. He, X. et al. Bendable ZnO thin film surface acoustic wave devices on polyethylene terephthalate substrate. *Appl. Phys. Lett.* **104**, 213504 (2014).
20. Chen, J. et al. Development of flexible ZnO thin film surface acoustic wave strain sensors on ultrathin glass substrates. *J. Micromech. Microeng.* **25**, 115005 (2015).

21. Xu, H. et al. Flexible surface acoustic wave strain sensor based on single crystalline LiNbO3thin film. *Appl. Phys. Lett.* **112**, 093502 (2018).
22. Lamanna, L., Rizzi, F., Giudo, F. & De Vittorio, M. Flexible Dual-Wave Mode AlN-Based Surface Acoustic Wave Device on Polymeric Substrate. *IEEE Electron Device Lett.* **41**, 1692–1695 (2020).
23. Ji, Z. et al. Flexible thin-film acoustic wave devices with off-axis bending characteristics for multisensing applications. *Microsyst. Nanoeng.* **7**, 97 (2021).
24. Jin, H. et al. Flexible surface acoustic wave respiration sensor for monitoring obstructive sleep apnea syndrome. *J. Micromech. Microeng.* **27**, 115006 (2017).
25. Nalamwar, A. L. & Epstein, M. Effects of Applied Strain in ZnO Thin-Film SAW Devices. *IEEE Trans. Sonics Ultrason* **23**, 144–147 (1976).
26. Nalamwar, A. L. & Epstein, M. Surface acoustic waves in strained media. *J. Appl. Phys.* **47**, 43–48 (1976).
27. Xu, H. et al. Flexible dual-mode surface acoustic wave strain sensor based on crystalline LiNbO3 thin film. *J. Micromech. Microeng.* **29**, 025003 (2019).
28. Lamanna, L. et al. Flexible and Transparent Aluminum-Nitride-Based Surface-Acoustic-Wave Device on Polymeric Polyethylene Naphthalate. *Adv. Electron. Mater.* **5**, 1900095 (2019).
29. Rodríguez-Madrid, J. G. et al. High precision pressure sensors based on SAW devices in the GHz range. *Sens. Actuators, A* **189**, 364–369 (2013).
30. Xiong, S. et al. Stability studies of ZnO and AlN thin film acoustic wave devices in acid and alkali harsh environments. *RSC Adv.* **10**, 19178–19184 (2020).
31. Lin, T. et al. Flow Analysis and Relative Humidity (RH) Measurement in the Horizontal Plane of a Front Opening Unified Pod (FOUP). *IEEE Trans. Semicond.* **34**, 429–435 (2021).
32. Anastasova, S. et al. A wearable multisensing patch for continuous sweat monitoring. *Biosens. Bioelectron.* **93**, 139–145 (2017).
33. Choi, J. W. et al. The influences of skin visco-elasticity, hydration level and aging on the formation of wrinkles: a comprehensive and objective approach. *Ski. Res Technol.* **19**, e349–e355 (2013).
34. Pang, Q. et al. Smart Flexible Electronics-Integrated Wound Dressing for Real-Time Monitoring and On-Demand Treatment of Infected Wounds. *Adv. Sci.* **7**, 1902673 (2020).
35. Zhang, Y. et al. Surface acoustic wave-based ultraviolet photodetectors: a review. *Sci. Bull.* **65**, 587–600 (2020).
36. Chevremont, A. C. et al. Impact of watering with UV-LED-treated wastewater on microbial and physico-chemical parameters of soil. *Water Res* **47**, 1971–1982 (2013).
37. Mori, M. et al. Development of a new water sterilization device with a 365 nm UV-LED. *Med Biol. Eng. Comput* **45**, 1237–1241 (2007).
38. Zhang, W., Zhang, L., Liao, Y. & Cheng, H. Conformal manufacturing of soft deformable sensors on the curved surface. *Int. J. Extrem. Manuf.* **3**, 042001 (2021).

ACKNOWLEDGEMENTS

This work was supported by the Excellent Youth Fund of Hunan Province (2021JJ20018), the NSFC (No. 52075162), the Program of New and High-tech Industry of Hunan Province (2020GK2015, 2021GK4014), the Joint Fund Project of the Ministry of Education, and the Engineering Physics and Science Research Council of UK (EPSRC EP/P018998/1) and International Exchange Grant (IEC/NSFC/201078) through Royal Society and the NSFC. We also thank the Sean Garner to provide the flexible glass and thank the Dr. Huamao Lin for the contribution to device's materials.

AUTHOR CONTRIBUTIONS

J.Z. and Z.J. conceived the original idea, designed the study, conducted the experiments and wrote the manuscript. Y.G. performed theoretical analysis and contributed to experimental analysis. Y.L. contributed to devices fabrication and analyzed device performance. F.Z. carried out the XRD, SEM and AFM measurements and were involved in drawing the graphs. Y.Z. analyzed and discussed the application results. Y.G. contributed to materials fabrication. Y.F. contributed to data analysis, paper writing and modifications. H.D. provided experimental platform, analyzed the experimental results and wrote the manuscript.

COMPETING INTERESTS

The authors declare no competing interests.

ADDITIONAL INFORMATION

Supplementary information The online version contains supplementary material available at https://doi.org/10.1038/s41528-022-00217-0.

Correspondence and requests for materials should be addressed to Huigao Duan.

Reprints and permission information is available at http://www.nature.com/reprints

Publisher's note Springer Nature remains neutral with regard to jurisdictional claims in published maps and institutional affiliations.